

Mediated Electrocatalysis with Polyanthraquinone-Functionalized Monolayer-Protected Clusters

Jeremy J. Pietron and Royce W. Murray*

Kenan Laboratories of Chemistry, University of North Carolina, Chapel Hill, North Carolina 27599-3290

Received: December 2, 1998; In Final Form: March 9, 1999

This paper describes the reduction of 1,1-dinitrocyclohexane by electrogenerated anthraquinone radical anions that are ligated to monolayer-protected gold clusters. Each cluster bears multiple (ca. 18) anthraquinone units. The clusters are prepared by place-exchange of a fraction of the cluster's original octanethiolate ligands with 1-(1,3-dithiapropryl)anthracene-9,10-dione. The electrocatalytic reduction currents are compared to those observed for anthraquinone monomer at an equivalent concentration. The electrocatalytic efficiency is larger for cluster-bound anthraquinone. The results are analyzed by digital simulation and by a discrete mathematical approach so as to determine the rate constant for electron transfer between the substrate and anthraquinone radical anion (cluster-bound and free). The rate constant is slightly larger for the free anthraquinone monomer. The enhancement in catalytic efficiency for cluster-bound anthraquinone arises from the smaller diffusion coefficient of cluster-bound anthraquinone, relative to that of the monomer, resulting in spatial compression of the reaction zone next to the electrode.

Introduction

The properties of nanometer-sized monolayer-protected clusters (MPCs), particularly those with gold cores, have been explored extensively in the past few years.¹ The electrochemical behavior of these materials is interesting because those with metal-like cores (>ca. 1.5 nm diameter) are, in effect, soluble nanoelectrodes. Such MPCs exhibit double layer capacitance charging at electrode interfaces² that, owing to their small individual capacitances, is observably quantized³ when the MPC sample is sufficiently monodisperse in core size. Reactivity of functional groups located at the outer edge of, as well as those buried deeply within, the monolayer has been explored.⁴ The MPCs can also be polyfunctionalized with redox groupings,⁵ using place exchange^{1d} or coupling⁶ reactions. The electron-transfer behavior of redox-MPCs can be expected to be analogous to that of dissolved redox polymers,⁷ with the added distinction that the redox-MPCs are more readily solubilized and the redox sites are spherically organized around the MPC core, much like a dendrimer polymer.⁸ The degree(s) of interaction between the MPC's redox sites, and indeed whether they are randomly distributed or not around the core, is not yet known.

The availability of redox-MPCs naturally raises possibilities for usefulness in mediated electrocatalysis, in which multiple copies of redox sites on each cluster are charged at an electrode and then deliver their redox equivalents to substrates in the solution. The MPCs offer further possibilities of building specific architectures into the monolayer so as to influence reaction rates through binding or electrostatic interactions with the substrate.

In this paper, we explore a first example of redox-MPC-mediated electrocatalysis. The example lacks any overt binding or electrostatic effects, and we mean simply to ask whether the rate of electron transfer delivery from a cluster-bound (anthraquinone) radical anion to a substrate (1,1-dinitrocyclohexane, DNC) is comparable to that from a radical anion not bound to

a cluster. The anthraquinone/DNC reaction is multielectron and previously characterized⁹ and was deemed a good model system for the present purposes. The reaction is shown in Scheme 1. In a preliminary observation,¹⁰ the cluster-bound anthraquinone (1-(1,3-dithiapropryl)anthracene-9,10-dione) seemed more reactive than monomer anthraquinone, at least as expressed by catalytic efficiency.¹¹ Catalytic efficiency, as defined in ref 11c, is the ratio of currents for catalytic mediator generator in the presence and absence of reaction substrate, normalized for the substrate/mediator concentration ratio. (Catalytic efficiency is defined somewhat differently in ref 11a). The detailed kinetic analyses presented here show that the rate constant for electron transfer from cluster-bound anthraquinone radical anion to 1,1-dinitrocyclohexane is actually slightly smaller than that for anthraquinone monomer. Drawing on previous observations^{11c} concerning effects of differing diffusion coefficients, the difference in catalytic efficiency is attributed to the slower diffusivity of cluster-bound anthraquinone, relative to the monomer.

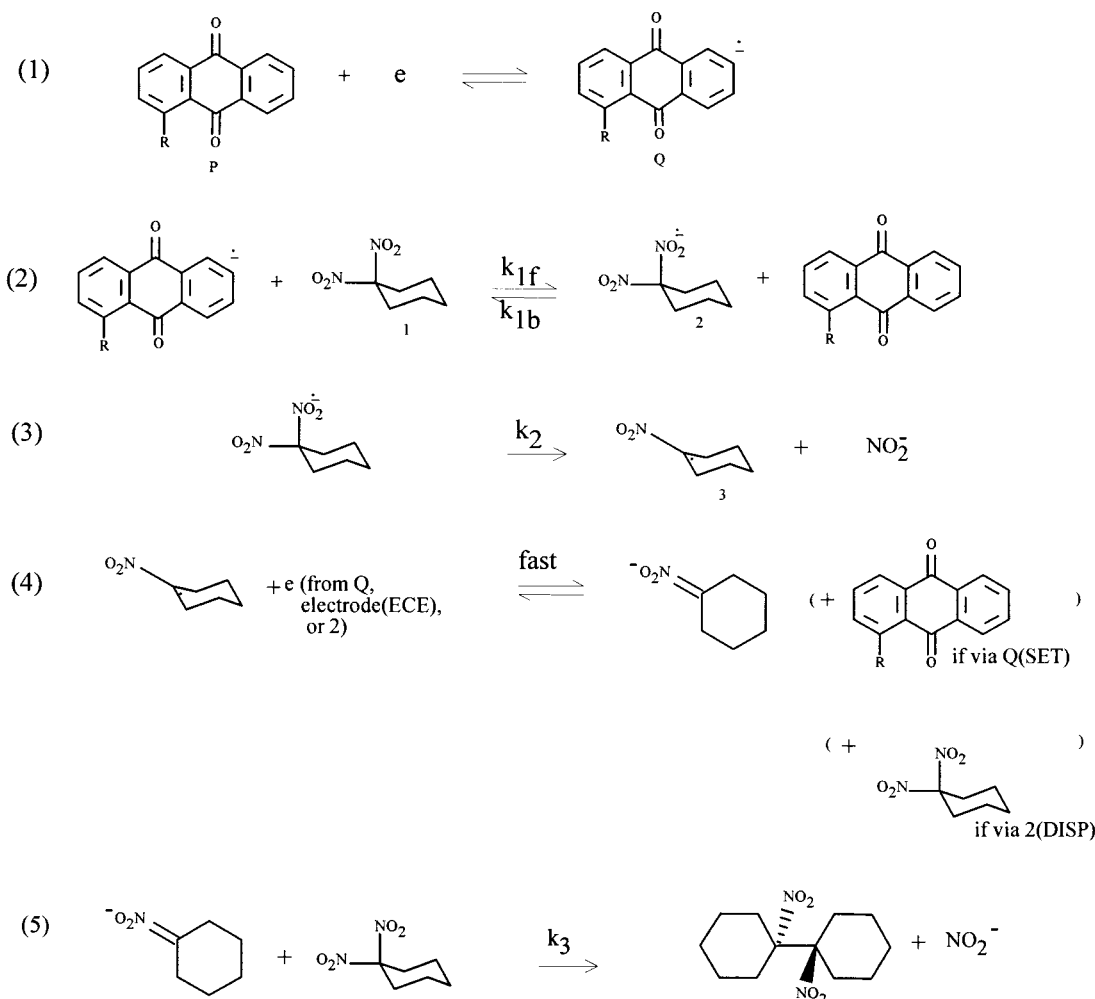
Experimental Section

Chemicals. HAuCl₄,¹² 1-(1,3-dithiapropryl)anthracene-9,10-dione,¹³ and 1,1-dinitrocyclohexane¹⁴ were synthesized according to literature methods. Tetraoctylammonium bromide (Aldrich), sodium borohydride (Johnson Matthey), toluene (Mallinckrodt), dimethylformamide (Mallinckrodt), absolute ethanol (AAPER), acetonitrile (Mallinckrodt), and octanethiol (Aldrich) were used as received. Tetrahexylammonium perchlorate (Hx₄-NClO₄, Alfa) was recrystallized from ethyl acetate (Fisher) and dried under vacuum at 40 °C. Ferrocene (EM Science) was sublimed before use.

Cluster Synthesis. Gold MPCs were synthesized^{1c} using a modified Brust reaction.^{1a} Briefly, AuCl₄⁻ (aqueous) was phase-transferred into toluene using tetraoctylammonium bromide, the aqueous phase was discarded, a 2-fold molar excess (relative to Au) of octanethiol was added to the mixture, and the reaction

SCHEME 1

R = H or SC3S-cluster



was allowed to proceed for 15 min. Then, an aqueous solution containing a 9-fold molar excess of sodium borohydride (relative to Au) was added dropwise over about 5 min at room temperature, completing the reduction of the gold. The solution quickly darkens during borohydride addition. After being stirred for 3 h, the water phase was discarded and the toluene was removed by rotary evaporation, leaving a black solid that was collected on a filter and washed copiously with absolute ethanol. On the basis of other studies,^{1c} these reaction conditions produce clusters that are modestly polydisperse in core sizes and have an *average* 2.0 nm core diameter. High-resolution transmission electron microscopy and modeling based on a truncated octahedral core shape suggest that the reaction produces a mixture of mainly 225 and 314 Au atom cores; we assume the latter. The assumption slightly affects values of cluster solution concentrations, but not their diffusion coefficients.^{2a} Thermogravimetric data indicate that such C8 MPCs contain about 91 octanethiolates in their protective monolayer shells.

Functionalization of the MPCs with AQSC3SH ligands was accomplished via place-exchange reactions,^{1d,10} in which $\text{CH}_2\text{-Cl}_2$ solutions containing 1-(1,3-dithiopropyl)anthracene-9,10-dione (AQSC3SH) and the C8 MPC in the desired mole ratio of AQSC3SH to octanethiolate chains were stirred for >24 h at room temperature. The AQSC3S/C8 MPC product was

precipitated by adding absolute ethanol, collected by filtration, washed with acetonitrile, and analyzed for relative AQSC3S and C8 ligand content by proton NMR. The 1:4 mole ratio obtained corresponds to an average of ca. 18 anthraquinone groups per cluster.

Measurements. Cyclic voltammetry was performed using a BAS 100B electrochemical workstation (Bioanalytical Systems). The working electrode was a 1.6 mm diameter Pt disk (Bioanalytical Systems) that was polished between experiments with 0.25 μm diamond paste (Buehler) and rinsed in water, DMF, and toluene. A Pt gauze and Ag wire served as counter and reference electrodes, respectively; the potential of the latter was referenced to the formal potential of the ferrocene/ferrocenium couple, which was added at submillimolar concentration. The 0.05 M $\text{Hx}_4\text{BuClO}_4$ in 2:1 (v/v) toluene/DMF solutions was degassed with solvent-saturated N_2 for >10 min and blanketed with solvent-soaked N_2 during experiments. The purpose of the toluene component was to secure adequate cluster solubility.

Digital Simulation. Experimental and simulated cyclic voltammograms (Digisim 2.1, Bioanalytical Systems) were compared based on best fits between their peak potentials and peak currents and, to a lesser extent, voltammetric waveshapes to produce rate constants (k_{1f}) for the reaction between anthraquinone radical anions and 1,1-dinitrocyclohexane.

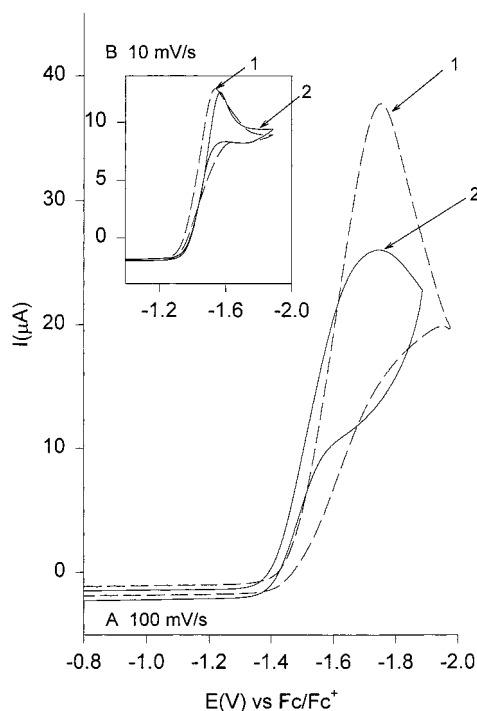


Figure 1. Cyclic voltammetry. Catalytic reduction of 5.75 mM 1,1-dinitrocyclohexane in 0.05 M HxNClO_4 /2:1 toluene/DMF at (A) 100 mV/s and (B) 10 mV/s. Curve 1 (A and B): mediation by 4:1 C8S/AQSC3S Au cluster. The solutions are 6.5 μM in cluster and therefore approximately 0.12 mM in cluster-bound anthraquinone. Curve 2: mediation of reduction by 0.12 mM free anthraquinone. The working electrode is a 1.6 mm Pt disk.

Results and Discussion

In the following experiments, the MPC concentrations used are 18-fold smaller than those of monomer anthraquinone, since each MPC bears an average of 18 anthraquinone sites. Providing equal overall concentrations of free and cluster-bound mediator facilitates comparison of the kinetics of the two forms in Scheme 1.

In Figure 1A, solutions containing equal concentrations of cluster-bound and monomer anthraquinone are compared in a potential sweep experiment at 100 mV/s. The electrocatalytic wave peak current appears at ca. -1.7 V versus the ferrocene internal reference potential. As reported in the preliminary experiment,¹⁰ the cluster solution (curve 1) produces the larger electrocatalytic peak current. This result can be expressed in terms of catalytic efficiency, which following Andrieux et al.,^{11c} we define as $i_p/2i_{pD}\gamma$, where i_p and i_{pD} are the peak currents for mediator (anthraquinone) with and without substrate and γ is the concentration ratio of substrate to mediator. The factor 2 accounts for the fact that the overall scheme is a two-electron process (Scheme 1). Catalytic efficiency in Figure 1A is 1.8 and 0.39 for the cluster-bound and monomer anthraquinone, respectively, and, as seen before,¹⁰ is substantially larger (by a factor of 4.5) for the cluster-bound anthraquinone. The source of the catalytic efficiency enhancement for the cluster-bound anthraquinone radical anion is a point of some interest. Electrocatalysts imbedded in Langmuir–Blodgett monolayers have exhibited increased activity, expressed as turnovers realized.¹⁵ In the present case, is the effect due to a larger rate constant for delivery of the initial (RDS) electron in reaction 2, Scheme 1, to the microscopically large local concentration of anthraquinone radical anions, to some binding-association of substrate to the cluster monolayer, or to some other factor?

TABLE 1: Rate Constant for Mediated Reduction of 1,1-Dinitrocyclohexane by the Radical Anion of 9,10-Anthraquinone^a

v (V/s)	$\gamma = 1.1$		$\gamma = 2.2$		$\gamma = 3.3$	
	k_{1f}	$\log k_{1f}$	k_{1f}	$\log k_{1f}$	k_{1f}	$\log k_{1f}$
Results from Digital Simulation ^b						
0.010	2.0×10^5	5.3	1.4×10^5	5.1	4.0×10^4	4.6
0.025	4.0×10^5	5.6	1.0×10^5	5.0	7.0×10^4	4.8
0.050	3.0×10^5	5.5	1.5×10^5	5.2	9.0×10^4	5.0
0.100	2.4×10^5	5.4	1.2×10^5	5.1	1.1×10^5	5.0
average	2.8×10^5	5.5	1.3×10^5	5.1	7.7×10^4	4.9
Results from eq 1 ^c						
	1.1×10^5	5.0	8.2×10^4	4.9	1.0×10^5	5.0

^a 0.1 mM anthraquinone, 2:1 toluene/DMF with 0.05M Hx_4NClO_4 at 298 K, concentrations of DNC for $\gamma = 1.1, 2.2$, and 3.3 are 0.12, 0.24, and 0.36 mM, respectively. ^b Values determined using digital simulation and reaction scheme shown in Scheme 1. ^c From the intercept of the plot of eq 1 in Figure 4.

The preceding question is partially resolved by recognizing that equal concentrations of cluster-bound and monomer anthraquinone yield quite different peak currents (i_p) in the absence of reaction substrate (not shown). That for monomer anthraquinone is ca. 3-fold larger because its voltammetrically determined diffusion coefficient, $1.5 \times 10^{-5} \text{ cm}^2/\text{s}$, is ca. 10-fold larger than that of cluster-bound anthraquinone, ca. $1.5 \times 10^{-6} \text{ cm}^2/\text{s}$. (Currents vary with the square root of diffusion coefficient.) Cluster-bound anthraquinone sites thus gain a catalytic efficiency advantage simply from their slower diffusion (relative to monomer) and their consequent electrocatalytic turnover in a thinner reaction volume at the electrode/solution interface. This effect has been predicted (see discussion^{11c} of “d”). Roughly a factor of 3-fold in the 4.5-fold catalytic efficiency advantage of the cluster in Figure 1A arises from the diffusion rate difference.

Figure 1B shows that catalytic efficiency also depends on the potential sweep rate. At a slower potential sweep rate (10 mV/s), the peak currents for the two kinds of anthraquinone mediator are now very similar. The catalytic efficiency for the cluster-bound anthraquinone (2.1) is, however, still larger than that of monomer anthraquinone (0.69). The ratio of the two, 3.0, is about that anticipated from the difference in diffusion rates noted above.

Two approaches were taken to the analysis of the rate constant k_{1f} for delivery of an electron from anthraquinone radical anion (monomer or cluster-bound) to DNC in reaction 2 of Scheme 1. In the first, the variations of electrocatalytic peak currents and potentials with solution and sweep rate parameters were compared to those digitally simulated for the reaction scheme for assumed values of k_{1f} and other reaction parameters either measured here or previously.⁹ The second approach, developed by Savéant and co-workers,¹¹ utilizes a closed-form mathematical solution to the electrochemical polarization problem which assumes kinetic control of the system strictly through k_{1f} . This approach is thought to be less exact since, according to the digital simulation results, Scheme 1 lies near the margin of this reaction zone behavior.

Kinetic Analysis Using Digitally Simulated Voltammetry. Experimental conditions employed for electrocatalytic reduction of DNC with monomer and cluster-bound anthraquinone mediators are indicated in Tables 1 and 2, respectively. These conditions, according to the study by Rühl and co-workers⁹ and inspection of Savéant’s kinetic zone diagrams^{11a} yield kinetic control of currents by the mediated electron-transfer step (reaction 2 in Scheme 1). The substrate concentrations employed

TABLE 2: Rate Constant for Mediated Reduction of 1,1-Dinitrocyclohexane by Cluster-Bound Anthraquinone Radical Anions^a

v (V/s)	$\gamma = 1.2$		$\gamma = 2.3$		$\gamma = 4.5$	
	k_{1f}	$\log k_{1f}$	k_{1f}	$\log k_{1f}$	k_{1f}	$\log k_{1f}$
Results from Digital Simulation ^b						
0.010	2.2×10^4	4.3	4.5×10^4	4.7	4.0×10^4	4.6
0.025	3.0×10^4	4.5	1.3×10^5	5.1	4.0×10^4	4.6
0.050	3.0×10^4	4.5	2.8×10^5	5.4	5.0×10^4	4.7
0.100	1.0×10^4	4.0			7.0×10^4	4.8
average	2.3×10^4	4.4	1.5×10^5	5.2	5.0×10^4	4.7
Results from eq 1 ^c						
	3.4×10^3	3.5	5.0×10^4	4.7	1.9×10^4	4.3

^a Concentration of 4:1 C8S/AQSC3S MPC is ca. 1×10^{-5} M, yielding an effective concentration of the 1-(1,3-dithiapropryl)anthracene-9,10-dione of 9.1×10^{-5} M. The solvent is 2:1(v/v) toluene/DMF with 0.05 Hx₄NCIO₄ as an electrolyte at 298 K and concentrations of DNC for $\gamma = 1.2, 2.3$, and 4.5 are 0.11, 0.21, and 0.41 mM, respectively. ^b Values determined using digital simulation and the mechanism shown in Scheme 1. ^c From the intercept of the plot of eq 1 in Figure 5.

(0.1–0.5 mM) are lower than those in Figure 1, as were concentration ratios of DNC substrate to anthraquinone catalyst ($\gamma = 1.2$ – 4.5 vs $\gamma = 5$ in Figure 1). The lower concentrations were for the purpose of working at smaller currents so as to ameliorate uncompensated potential losses (iR_{UNC}) in the resistive toluene/DMF solvent. 2–3 k Ω values of R_{UNC} in Figure 1, for example, cause 30 mV distortions in peak potential measurements; iR_{UNC} distortions of measured peak potentials are small enough at 0.1–0.5 mM substrate concentrations to avoid substantive effect on the Table 1 and 2 rate constant evaluations.

Scheme 1 requires input of several parameters besides k_{1f} which were arrived at as follows. First, we assumed $k_2 = 1.6 \times 10^6$ s⁻¹, based on the report⁹ by Rühl et. al. of $k_2 = 1.6 \times 10^6$ and 1.1×10^6 s⁻¹ in DMF and water, respectively. k_{1b} is assumed to be under diffusion control and is estimated to be on the order of 10^9 M⁻¹ s⁻¹. Values of peak currents and potentials and of k_{1f} are relatively insensitive to k_2 ; 10-fold changes have little effect on simulated values. Second, the second reduction step (reaction 4 in Scheme 1), whether occurring at the electrode (ECE reaction¹⁶), with anthraquinone radical anion mediator (SET reaction¹⁷), or via disproportionation with the dinitrocyclohexane radical anion (DISP 1¹⁶), is assumed to be fast and under diffusion control. Third, we assumed $k_3 = 10^3$ M⁻¹ s⁻¹ (reaction 5 in Scheme 1), again following Rühl et. al.⁹ Fourth, comparisons between experimental and simulated voltammograms for monomer and cluster-bound anthraquinone electrocatalysis of dinitrocyclohexane reduction in toluene/DMF give a DNC^{0/-} formal potential of -1.67₅ V vs Fc^{+/0}. This potential is more negative than that (-1.53 V vs Fc^{+/0}) observed by Rühl et al.⁹ in DMF solvent, but those of monomer (-1.42 V) and cluster-bound (-1.41 V) anthraquinone^{0/-} in toluene/DMF are also shifted and by similar amounts (Rühl et al.⁹ measured -1.31 V vs Fc^{0/+} in DMF). The less polar toluene/DMF solvent is, unsurprisingly, a poorer solvent for the dinitrocyclohexyl and the anthraquinone radical anions. Finally, oxidation of the nitrite product of reactions 3 and 5 and reduction of the dimer produced in reaction 5 are assumed to occur at potentials outside the range affecting the electrocatalytic process.

The upper sections of Tables 1 and 2 list rate constants evaluated for electrocatalysis with monomer and cluster-bound anthraquinone, respectively. Results for monomer anthraquinone (Table 1, upper), averaging $\log k_{1f} = 5.1 \pm 0.3$ M⁻¹ s⁻¹, are within experimental uncertainty, identical to that, $\log k_{1f} = 5.0$

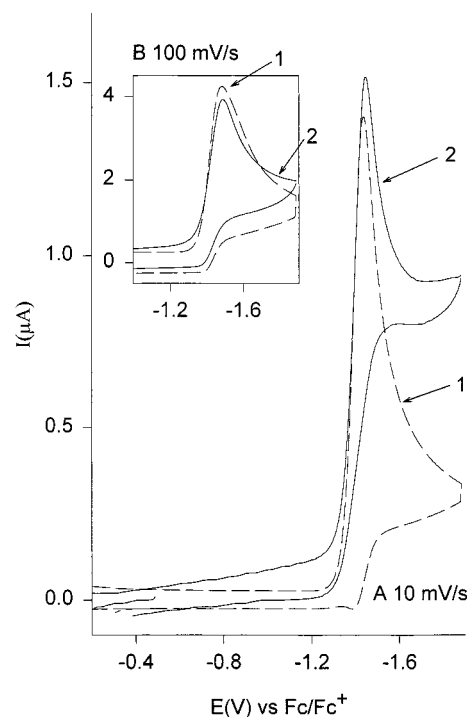


Figure 2. Cyclic voltammetry and digital simulation. Catalytic reduction of 0.36 mM 1,1-dinitrocyclohexane in 0.05 M Hx₄NCIO₄/2:1 toluene/DMF by 0.11 mM free anthraquinone; $\gamma = 3.5$. (A) 10 mV/s. Curve 1 is the simulated result. Curve 2 is the experimental data. Fitting of the peak potential to the forward rate constant k_{1f} yields $k_{1f} = 4 \times 10^4$ M⁻¹ s⁻¹. (B) Same as (A) but at 100 mV/s. Again, curve 1 is the simulated result, and curve 2 is the experimental data. Fitting of the peak potential to the forward rate constant yields $k_{1f} = 1.1 \times 10^5$ M⁻¹ s⁻¹.

± 0.2 M⁻¹ s⁻¹, reported previously.⁹ The average result, $\log k_{1f} = 4.7 \pm 0.4$ M⁻¹ s⁻¹, for cluster-bound anthraquinone (Table 2, upper) under comparable conditions is somewhat lower than that for monomer anthraquinone. The difference in the overall averages comes mainly from the data at $\gamma = 1.2$; the monomer and cluster-bound anthraquinone $\log k_{1f}$ are in better agreement at the larger excess factors (averages 5.0 and 4.8, respectively). We conclude from the k_{1f} results that the electron transfer dynamics of anthraquinone radical anions that are bound to nanoscopic clusters, while slightly slower, approach rather closely those of monomer anthraquinone radical anions, in their reaction with dinitrocyclohexane.

The rate constants in Tables 1 and 2 (upper) were based mainly on comparisons of experimental and simulated peak potentials and how they varied with potential sweep rate and concentrations. Figures 2 and 3 show comparisons of real and simulated data for some example electrocatalytic reductions using monomer and cluster-bound anthraquinone mediators, respectively. Choosing the rate constants such that peak potentials exactly matched produces reasonably good agreement between simulation and experiment for peak currents and wave shape, especially at the larger potential sweep rates. At slower potential sweep rates, the experimental peak currents tend to be larger, since the reduction wave, as seen most clearly from the appearance of the post-peak current tail, "rides" on an increasing background current that is in part due to trace oxygen reduction. Experiments conducted in the absence of substrate confirm this. Other uncertainties in the comparisons include, for cluster-bound anthraquinone, those in cluster diffusion coefficients, in the NMR-based analysis of clusters for the average number of anthraquinones/cluster, in subtracting the double-layer charging of the cluster cores that imposes sloping

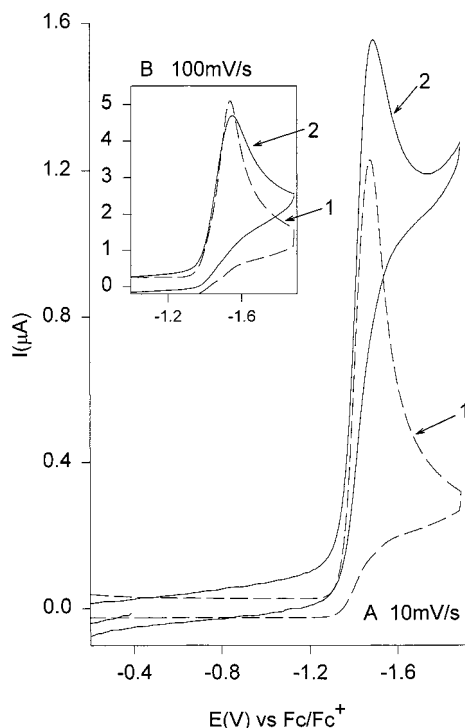


Figure 3. Cyclic voltammetry and digital simulation. Catalytic reduction of 0.43 mM 1,1-dinitrocyclohexane in 0.05 M Hx_4NClO_4 /2:1 toluene/DMF by 0.09 mM cluster-bound anthraquinone; $\gamma = 4.8$. (A) 10 mV/s. Curve 1 is the simulated result. Curve 2 is the experimental data. Fitting of the peak potential to the forward rate constant k_{if} yields $k_{\text{if}} = 4 \times 10^4 \text{ M}^{-1} \text{ s}^{-1}$. (B) Same as (A) but at 100 mV/s. Again, curve 1 is the simulated result, and curve 2 is the experimental data. Fitting of the peak potential to the forward rate constant yields $k_{\text{if}} = 7 \times 10^4 \text{ M}^{-1} \text{ s}^{-1}$.

baselines in their voltammetry,^{1c,2} and the tendency of clusters to physisorb on electrodes to varying extents.^{2b} Given these inherent challenges, the relatively good agreement of rate constants for the cluster-bound and monomer anthraquinone reactions is viewed as respectable.

Analysis Using a Semiclosed Form Relation. Savéant and co-workers have described a series of differential equations and their closed, numerically determined integral solutions for the (a) direct ECE reaction¹⁶ and mediated multielectron reactions, with mediator diffusion coefficient values approximately the (b) same as^{11a} and (c) considerably different^{11c} from the substrate. Case (c) is the more general of the mediated electron-transfer schemes, and we applied it to mediation by monomer anthraquinone and by cluster-bound anthraquinone.

The original expression^{11c} was cast in dimensionless parameters; re-expressing it as a relation between cyclic voltammetry peak potential for an ECE reaction with a chemical rate constant k_1 ,

$$E_p - E^\circ = RT/F \{ \ln[1/v] + \ln[(RT/F)(k_1 C_p^\circ / 2\gamma d^{1/2})] - 0.125 \} \quad (1)$$

where k_1 refers to the electron-transfer reaction between mediator and substrate (reaction 2, k_{if} , Scheme 1), v is the potential sweep scan rate, E_p is the measured peak potential, E° is the standard potential for the mediator, γ is ratio of substrate and mediator concentrations, C_p° is the bulk concentration of the mediator, and d is the ratio of mediator and substrate diffusion coefficients. This equation is adapted to the two-electron reaction in Scheme 1 by doubling the value of γ used in the computation, so in the

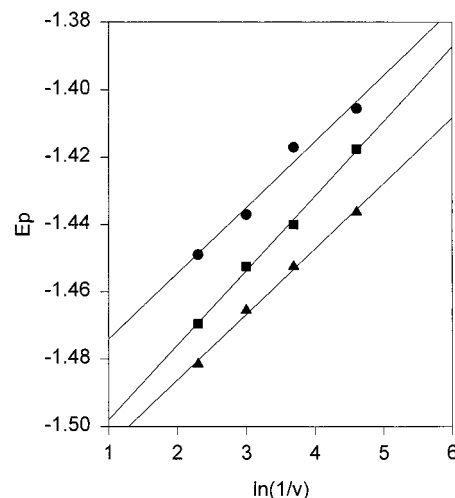


Figure 4. Cyclic voltammetry. Plot of catalytic peak potential, E_p , versus the logarithm of $1/(\text{sweep rate})$ for catalytic reduction of 0.12 mM (●), 0.24 mM (■) and 0.36 mM (▲) 1,1-dinitrocyclohexane by 0.11 mM anthraquinone in 0.05 M Hx_4NClO_4 /2:1 toluene/DMF. Slopes of the plots are 19.6, 22.2, and 19.5 mV, respectively. Analysis of the intercepts yields forward rate constants, k_{if} , of $1.1 \times 10^5 \text{ M}^{-1} \text{ s}^{-1}$, $8.2 \times 10^4 \text{ M}^{-1} \text{ s}^{-1}$ and $1.0 \times 10^5 \text{ M}^{-1} \text{ s}^{-1}$.

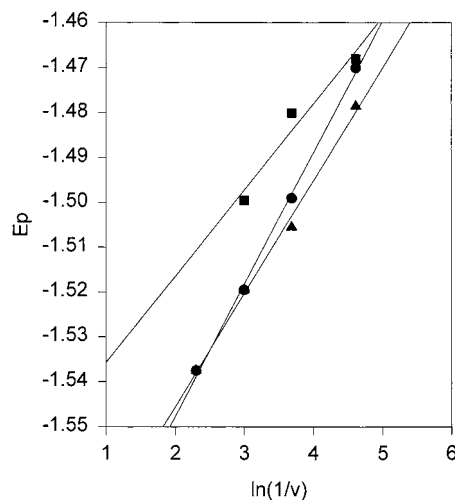


Figure 5. Cyclic voltammetry. Plot of catalytic peak potential, E_p , versus the logarithm of $1/(\text{sweep rate})$ for catalytic reduction of 0.1 mM (●), 0.21 mM (■), and 0.41 mM (▲) 1,1-dinitrocyclohexane by ca. $5 \mu\text{M}$ 4:1 C8S/AQSC3S Au cluster (ca. 0.09 mM cluster-bound anthraquinone) in 0.05 M Hx_4NClO_4 /2:1 toluene/DMF. Slopes of the plots are 29.3, 19.2, and 25.1 mV, respectively. Analysis of the intercepts yields forward rate constants, k_{if} , of $3.14 \times 10^3 \text{ M}^{-1} \text{ s}^{-1}$, $5.0 \times 10^4 \text{ M}^{-1} \text{ s}^{-1}$ and $1.9 \times 10^4 \text{ M}^{-1} \text{ s}^{-1}$.

specific case of Scheme 1, a denominator of $4\gamma d^{1/2}$ in the logarithmic portion of the equation is appropriate.

Equation 1 indicates that plots of experimental peak potential vs v^{-1} should at 298 K be linear with 25.7 mV slopes and intercepts of $[E^\circ + (0.0257 \text{ V}) \{ \ln [(0.0257 \text{ V})(k_1 C_p^\circ / 4\gamma d^{1/2})] - 0.125 \}]$ from which k_1 can be extracted. Figures 4 and 5 compare experimental peak potentials to eq 1 for, respectively, reduction of dinitrocyclohexane by monomer and cluster-bound anthraquinone radical anion. The peak potential data are the same as were compared to digital simulations, and the experimental conditions are those in Tables 1 and 2. The results for k_1 are given in Tables 1 and 2, lower. Comparing the Table 1 (lower) results from eq 1 and Figure 4 to those obtained by the digital simulation approach (Table 1, upper) for DNC reduction by monomer anthraquinone radical anion, the agreement is excellent, and well within the estimated uncertainties of experi-

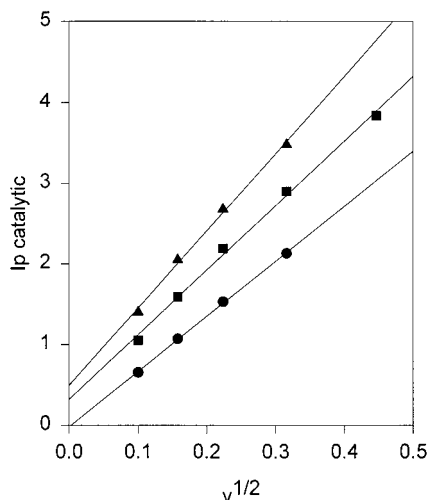


Figure 6. Plot of catalytic currents versus (voltage sweep rate)^{1/2} for catalytic reduction of DNC by ca. 0.11 M anthraquinone. The substrate concentrations are 0.12, 0.24, and 0.36 mM ($\gamma = 1.1, 2.2, 3.3$) for the lower, middle, and upper plots, respectively. Slopes of the plots in amperes-s^{1/2}/V^{1/2} are 6.8, 8.0 and 9.6 ($\times 10^{-6}$). The electrode and electrolyte are the same as in experiments described in Figures 1–3.

ment and analysis. The same comparison for the DNC reduction by cluster-bound anthraquinone radical anion shows that the Figure 5 results at the two larger excess factors (γ) are in fairly good agreement with those obtained by digital simulation comparisons (Table 2). By both analyses, the Table 2 k_{if} results at small γ suggest a slower reaction rate there.

The slopes of the plots in Figures 4 (19.6, 22.1, and 19.5 mV) and 5 (29.3 mV, 19.2 mV and 25.2 mV) are somewhat scattered and tend collectively to be smaller than the ideal 25.7 mV. Equation 1 strictly speaking applies to situations where the reaction rate is controlled solely by the diffusion rate of the substrate to the reaction layer, and the effect of mediated reaction shows up in the peak potential rather than the peak current, which should be proportional to $v^{1/2}$ and to substrate concentration. Figures 6 and 7 are plots of catalytic peak current versus $v^{1/2}$ for reduction of DNC by monomer and cluster-bound anthraquinone, respectively. In the case of control of the reaction by the forward rate constant alone, and thus by diffusion of the substrate to the reaction layer, the peak currents are described by¹⁶

$$i_{p,\text{catalytic}} = 0.430(2^{1/2})FAC_A^\circ D_A^{1/2}(Fv/RT)^{1/2} \quad (2)$$

where A is electrode area, C_A° is the concentration of the substrate, and D_A is the substrate diffusion coefficient. The plots seem to be roughly linear, but the slopes are instructive in that they do not scale exactly linearly with substrate concentration and develop nonzero intercepts (or curvature) at large γ . In Figure 6, for substrate concentrations of 0.12, 0.22, and 0.46 mM, the ratios of slopes to substrate concentrations are 37, 37, and 25 ($\times 10^{-6}$ amperes s^{1/2}/V^{1/2} mM), respectively. These slight deviations from linearity suggest that the rate of the back electron transfer (in reaction 2, k_{1b}) may be significant so that the reaction is under “mixed control”^{11a} and violates somewhat the premises of eqs 1 and 2. In Figure 7, the effect is even more noticeable; at substrate concentrations of 0.12, 0.24, and 0.36 mM, the ratios of slopes to substrate concentrations are 57, 33, and 27 ($\times 10^{-6}$ amperes s^{1/2}/V^{1/2} mM), respectively. The digital simulation results and a Savéant kinetic zone diagram^{11a} imply that this may be the case. This approximate aspect of eq

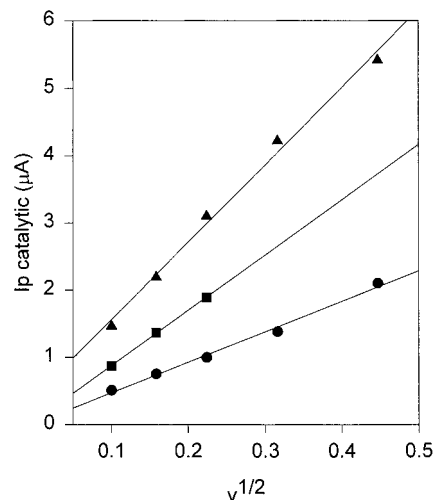


Figure 7. Plot of catalytic currents versus (voltage sweep rate)^{1/2} for catalytic reduction of DNC by ca. 5 μ M 4:1 C8S/AQSC3S MPC. The effective concentration of anthraquinone is 0.09 mM. The substrate concentrations are 0.11, 0.21, and 0.41 mM ($\gamma = 1.2, 2.3, 4.5$) for the lower, middle, and upper plots, respectively. Slopes of the plots in amperes-s^{1/2}/V^{1/2} are 4.5, 8.2, and 11.5 ($\times 10^{-6}$). The electrode and electrolyte are the same as in experiments described in Figures 1–3.

1 may cause the slope deviations in Figures 4 and 5. For these reasons, we regard the digital simulation of analysis of the rate constant k_{if} as the more reliable.

Conclusions

Analysis of the electrocatalytic experiments has shown that (a) radical anions of anthraquinone bound to monolayer-protected metal clusters can be used as electron transfer mediators in the same manner as monomeric anthraquinone radical anions, and (b) that their reaction rates are nearly as fast as those of the monomeric species. This is an element of predictivity of chemical reactivity that is analogous to that observed (in general) for chemically modified electrodes;¹⁸ that is, the present result suggests that design of MPC monolayers for electrocatalysis may be guided by the literature storehouse of knowledge about homogeneous solution reactions of monomeric mediators. This is a significant result of this first example of MPC mediator-catalyst kinetics.

What else do the reaction results show? Comparison of Figure 1 with the rate constant results of Tables 1 and 2 show that the cluster-bound anthraquinone radical anion can produce larger electrocatalytic currents than monomer anthraquinone, but that this difference is *not* caused by a faster electron-transfer rate constant. The current difference seen in Figure 1 is a consequence, it would seem, solely of the slower rate at which cluster-bound anthraquinones (relative to monomers) diffuse to and away from the generating electrode. (The general effect has been predicted.^{11c}) Qualitatively, this produces a compression of the reaction zone for DNC reduction, steeper fluxes of mediator and substrate, and decreased likelihood for a role of the diffusion-controlled back reaction. Again there is an analogy of thinned reaction zones with the properties of chemically modified electrodes, in which catalytic reaction flux is maximized by a monolayer of catalyst that does not diffuse at all but is attached to the electrode surface.^{18b}

Finally, the present results do not probe the special attributes for electrocatalysis that we believe may be possible by further research on MPCs, such as designed, reversible binding of reaction substrate to the polyelectron D/A MPC center.

Acknowledgment. This research was supported in part by grants from the National Science Foundation and the Office of Naval Research.

References and Notes

- (1) (a) Brust, M.; Walker, M.; Bethell, D.; Schiffrin, D. J.; Whyman, R. *J. Chem. Soc., Chem. Commun.* **1994**, 801–802. (b) Terrill, R. H.; Postlethwaite, T. A.; Chen, C.-h.; Poon, C.-D.; Terzis, A.; Chen, A.; Hutchison, J. E.; Clark, M. R.; Wignall, G.; Londono, J. D.; Superfine, R.; Falvo, M.; Johnson, C. S., Jr.; Samulski, E. T.; Murray, R. W. *J. Am. Chem. Soc.* **1995**, *117*, 12537–12548. (c) Hostetler, M. J.; Wingate, J. E.; Zhong, C.-J.; Harris, J. E.; Vachet, R. W.; Clark, M. R.; Londono, J. D.; Green, S. J.; Stokes, J. J.; Wignall, G. D.; Glish, G. L.; Porter, M. D.; Evans, N. D.; Murray, R. W. *Langmuir* **1998**, *14*, 17–30. (d) Hostetler, M. J.; Green, S. J.; Stokes, J. J.; Murray, R. W. *J. Am. Chem. Soc.* **1996**, *118*, 4212–4213. (e) Hostetler, M. J.; Murray, R. W. *Curr. Opin. Colloid Interface Sci.* **1997**, *2*, 42–50 and references therein.
- (2) (a) Green, S. J.; Stokes, J. J.; Hostetler, M. J.; Pietron, J. J.; Murray, R. W. *J. Phys. Chem. B* **1997**, *101*, 2663–2668. (b) Green, S. J.; Pietron, J. J.; Stokes, J. J.; Hostetler, M. J.; Vu, H.; Wuelfing, W. P.; Murray, R. W. *Langmuir* **1998**, *14*, 5612–5619.
- (3) (a) Ingram, R. S.; Hostetler, M. J.; Murray, R. W.; Schaaf, T. G.; Khoury, J. T.; Whetten, R. L.; Bigioni, T. P.; Guthrie, D. K.; First, P. N. *J. Am. Chem. Soc.* **1997**, *119*, 9279–9286. (b) Chen, S.; Ingram, R. S.; Hostetler, M. J.; Pietron, J. J.; Murray, R. W.; Schaaf, T. G.; Khoury, J. T.; Alvarez, M. M.; Whetten, R. L. *Science* **1998**, *280*, 2098–2101.
- (4) Templeton, A. C.; Hostetler, M. J.; Kraft, C. T.; Murray, R. W. *J. Am. Chem. Soc.* **1998**, *120*, 1906–1911.
- (5) Ingram, R. S.; Hostetler, M. J.; Murray, R. W. *J. Am. Chem. Soc.* **1997**, *119*, 9175–9178.
- (6) Templeton, A. C.; Hostetler, M. J.; Warmoth, E. K.; Chen, S.; Hartshorn, C. M.; Krishnamurthy, V. M.; Forbes, M. D. E.; Murray, R. W. *J. Am. Chem. Soc.* **1998**, *120*, 4845–4849.
- (7) (a) Jehoulet, C.; Bard, A. J. *J. Am. Chem. Soc.* **1991**, *113*, 5456–5457. (b) Flanagan, J. B.; Margel, S.; Bard, A. J.; Anson, F. C. *J. Am. Chem. Soc.* **1978**, *100*, 248.
- (8) Newkome, G. R.; Moorefield, C. N.; Vögtle, F. *Dendritic Molecules: Concepts, Synthesis, Perspectives*; VCH: New York, 1996.
- (9) Rühl, J. C.; Evans, D. H.; Hapiot, P.; Neta, P. *J. Am. Chem. Soc.* **1991**, *113*, 5188–5194.
- (10) Ingram, R. S.; Murray, R. W. *Langmuir* **1998**, *14*, 4115–4121.
- (11) (a) Andrieux, C. P.; Dumas-Bouchiat, J. M.; Savéant, J. M. *J. Electroanal. Chem.* **1980**, *113*, 1–18. (b) Andrieux, C. P.; Blocman, C.; Dumas-Bouchiat, J. M.; M'Halla, F.; Savéant, J. M. *J. Electroanal. Chem.* **1980**, *113*, 19–40. (c) Andrieux, C. P.; Hapiot, P.; Savéant, J. M. *J. Electroanal. Chem.* **1985**, *189*, 121–133.
- (12) (a) *Handbook of Preparative Inorganic Chemistry*; Brauer, G., Ed.; Academic Press: New York, 1965; pp 1054–1059. (b) Block, B. P. *Inorg. Synth.* **1953**, *4*, 14–17.
- (13) Zhang, L.; Lu, T.; Gokel, G. W.; Kaifer, A. E. *Langmuir* **1993**, *9*, 786–791.
- (14) Kaplan, R. R.; Schechter, H. J. *J. Am. Chem. Soc.* **1961**, *83*, 3535–3536.
- (15) Töllner, K.; Popovitz-Biro, R.; Lahaiv, M.; Milstein, D. *Science* **1997**, *278*, 2100–2102.
- (16) Amatore, C.; Savéant, J. M. *J. Electroanal. Chem.* **1977**, *85*, 27–46.
- (17) Savéant, J. M.; Su, K. B. *J. Electroanal. Chem.* **1985**, *196*, 1–22.
- (18) See, for examples (and references therein): (a) Murray, R. W.; Ewing, A. G.; Durst, R. A. *Anal. Chem.* **1987**, *1987*, 379A–390A. (b) Andrieux, C. M.; Savéant, J. M. In *Molecular Design of Electrode Surfaces*; Murray, R. W., Ed.; Techniques of Chemistry; Wiley-Interscience: New York, 1992; Vol. XXII. (c) Murray, R. W. In *Electroanalytical Chemistry*; Bard, A. J., Ed.; Marcel Dekker: New York, 1984; pp 192–368.